Combination of Forced Diuresis with Additional Late Imaging in ^{68}Ga-PSMA-11 PET/CT: Effects on Lesion Visibility and Radiotracer Uptake

Ian Alberts[1], Jan Niklas-Hünermund[1], Christos Sachpekidis[1], Helle Damgaard Zacho[2], Clemens Mingels[1], Lotte Dijkstra[1], Karl Peter Bohn[1], Tilman Läppchen[1], Eleni Gourni[1], Axel Rominger[1], and Ali Afshar-Oromieh[1]

[1]*Department of Nuclear Medicine, Inselspital, Bern University Hospital, University of Bern, Bern, Switzerland; and* [2]*Aalborg University Hospital, Universitetshospital, Aalborg, Denmark*

Renal excretion of some prostate-specific membrane antigen (PSMA) ligands and consequently increased bladder activity can obscure locally relapsing prostate cancer lesions in PSMA PET/CT. Furthermore, additional late imaging in PSMA PET/CT provides a useful method to clarify uncertain findings. The aim of this retrospective study was to investigate a modified imaging protocol combining late additional imaging with hydration and forced diuresis in individuals undergoing additional late scanning for uncertain lesions or low prostate-specific antigen. **Methods:** We compared an older protocol with a newer one. In the old protocol, patients undergoing ^{68}Ga-PSMA-11 PET/CT were examined at 90 min after injection, with 1 L of oral hydration beginning at 30 min after injection and 20 mg of furosemide given intravenously at 1 h after injection, followed by additional late imaging at 2.5 h after injection without further preparation. In the new protocol, a second group received the same procedure as before, with an additional 0.5 L of oral hydration and 10 mg of furosemide intravenously 30 min before the late imaging. We examined 132 patients (76 with the old protocol and 56 with the new one) with respect to urinary bladder activity (SUV_{mean}), prostate cancer lesion uptake (SUV_{max}), and lesion contrast (ratio of tumor SUV_{max} to bladder SUV_{mean} for local relapses and ratio of tumor SUV_{max} to gluteal-muscle SUV_{mean} for nonlocal prostate cancer lesions). **Results:** Bladder activity was significantly greater for the old protocol in the late scans than for the new protocol (ratio of bladder activity at 2.5 h to bladder activity at 1.5 h, 2.33 ± 1.17 vs. 1.37 ± 0.50, $P < 0.0001$). Increased tumor SUV_{max} and contrast were seen at 2.5 h compared with 1.5 h ($P < 0.0001$ for old protocol; $P = 0.02$ for new protocol). Increased bladder activity for the old protocol resulted in decreased lesion-to-bladder contrast, which was not the case for the new protocol. Tumor-to-background ratios increased at late imaging for both protocols, but the increase was significantly lower for the new protocol. For the old protocol, comparing the 1.5-h to the 2.5-h acquisitions, 4 lesions in 4 patients (4/76 = 5.2% of the cohort) were visible at the postdiuresis 1.5-h acquisition but not at 2.5 h, having been obscured as a result of the higher bladder activity. In the new protocol, 2 of 56 (3.6%) patients had lesions visible only at late imaging, and 2 patients had lesions that could be better discriminated at late imaging. **Conclusion:** Although the combination of diuretics and hydration can be a useful method to increase the visualization and detectability of locally recurrent prostate cancer in standard ^{68}Ga-PSMA-11 PET/CT, their effects do not sufficiently continue into additional late imaging. Additional diuresis and hydration are recommended to improve the visibility, detection, and diagnostic certainty of local recurrences.

Key Words: PSMA; furosemide; diuresis; dual-time point; hydration

J Nucl Med 2021; 62:1252–1257
DOI: 10.2967/jnumed.120.257741

For recurrent prostate cancer, ^{68}Ga-PSMA-11 PET/CT has become the examination of choice, with excellent tumor-to-background contrast and high sensitivity (*1*). However, ^{68}Ga-PSMA-11, in common with other prostate-specific membrane antigen (PSMA) radioligands such as ^{18}F-DCFPyl, undergoes predominantly renal excretion (*2,3*). Activity in the urinary bladder can obscure locally recurrent lesions, which are at risk of being missed (*4*). PET/MRI and PET/CT are vulnerable to the halo artifact with large activity concentrations in the urinary bladder (*5,6*), although this can be minimized by adequate scatter correction. Novel radiotracers that undergo biliary excretion have been introduced, which when labeled with ^{18}F combine the advantages of cyclotron production of the radiotracer and improved availability, longer half-life, and reduced bladder activity (*7,8*).

Despite nearly a decade of routine use, the optimal examination protocol for PSMA radiotracers remains elusive, with only generic guidance available (*9*). PET/CT with ^{68}Ga-PSMA-11 is commonly performed at 1 h after injection. However, several publications show an increase in tracer uptake for most prostate cancer lesions over time (*2,10–13*). Later acquisition of images or additional late imaging can improve lesion visibility and aid in the discrimination of tracer uptake not related to prostate cancer (*12*).

Several publications report the utility of forced diuresis as a means of mitigating urinary bladder activity and improving diagnostic certainty for lesions near the bladder and ureters (*14*). The extant guidelines recommend application of furosemide either shortly before or after administration of ^{68}Ga-PSMA-11 (*9*), although early coapplication of radiotracer and diuretic is associated with degraded image quality at delayed imaging (*15*). Instead, later application is associated with improved lesion detection and reduced bladder activity (*16*). In cases of uncertain findings, later imaging may better discriminate between pathologic and nonpathologic causes of tracer uptake; most tumor lesions exhibit increasing PSMA ligand uptake, whereas ganglia or inflammatory lymph nodes usually do not (*17,18*). Whereas previous studies

Received Oct. 5, 2020; revision accepted Dec. 28, 2020.
For correspondence or reprints, contact Ali Afshar-Oromieh (ali.afshar@insel.ch).
Published online February 5, 2021.

examined the optimal imaging time point for ^{68}Ga-PSMA-11 (*19*), with increased lesion detection when combining later imaging (at 90 min vs. 60 min after injection) with diuresis (*20*), no publications, to our knowledge, have systematically addressed the issue of dual-time-point imaging and forced diuresis. Furthermore, we know of no studies that have reported the influence of diuresis on tumor uptake, which this study aimed to address.

MATERIALS AND METHODS

In this retrospective analysis, we investigated 132 individuals who, having been referred to our center for biochemically recurrent prostate cancer between October 2018 and October 2019, underwent ^{68}Ga-PSMA-11 PET/CT including additional late imaging. The cantonal ethics committee approved this retrospective study (KEK number 2020-00162), and the requirement to obtain informed consent was waived. The study was performed in accordance with the declaration of Helsinki. Starting in 2018, our institutional protocol was to perform PET/CT with ^{68}Ga-PSMA-11 at 90 min after injection, with 20 mg of intravenous furosemide given at 60 min after injection and 1 L of water taken by mouth beginning at 30 min after injection. Additional late scans were acquired at 2.5 h after injection in cases of low prostate-specific antigen (<2.0 ng/mL) or when uncertain lesions were identified on the whole-body PET images, as previously published (*10*). In the old, 2018, protocol, this late imaging was performed without any further preparation and was as previously published (*20*). Noting increased bladder activity at late imaging compared with the regular scans, our protocol changed in April 2019 to a new one that includes additional furosemide (10 mg intravenously) at 2 h after injection and 0.5 L of water by mouth before late imaging at 2.5 h after injection. The 2 examination protocols are as outlined in Figure 1. Our analysis compared 76 consecutive patients who were imaged according to the old protocol with 56 consecutive patients who were imaged according to the new protocol (until October 2019, when we switched to the routine use of a ^{18}F-PSMA tracer). Patient details, including prior treatments for both cohorts, Gleason score, and prostate-specific antigen level, are outlined in Table 1.

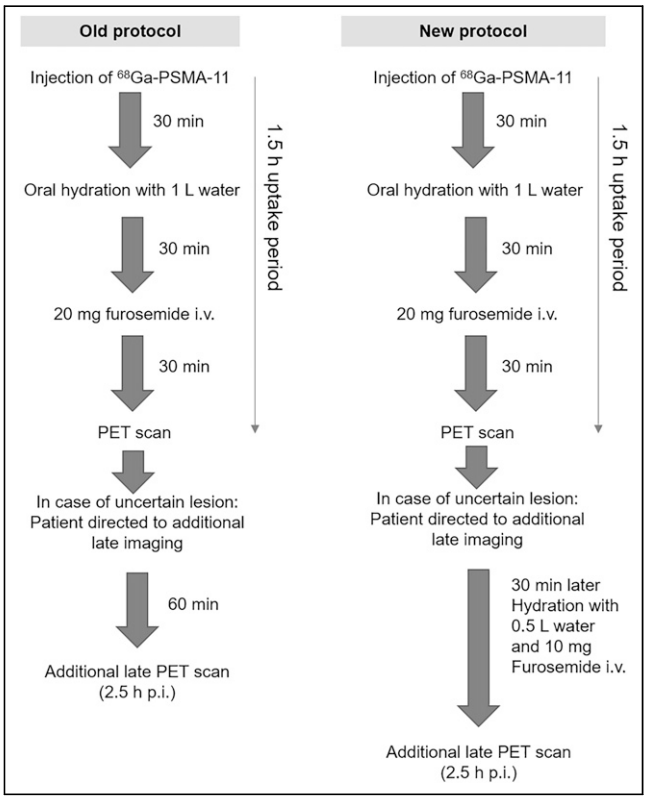

FIGURE 1. Comparison of old and new protocols. p.i. = after injection; i.v. = intravenously.

Radiotracer

^{68}Ga-PSMA-11 was produced as previously described (*21,22*) and given as an intravenous bolus injection with a standard body weight–adjusted dose of 2–3 MBq/kg.

Imaging

All patients received regular whole-body PET scans (from head to thighs) at 1.5 h after injection. Additional late imaging was performed at 2.5 h after injection. Hydration and forced diuresis for both groups were as outlined in Figure 1. Patients were asked to void the bladder immediately before all imaging. Both the 1.5-h and the 2.5-h scans were analyzed for pathologic lesions characteristic of prostate cancer and for the activity concentration in the urinary bladder. Our PET and CT protocol parameters were as previously published (*23*).

Image Evaluation

Images were analyzed using an appropriate workstation and software (SyngoVia; Siemens). Two experienced physicians read each dataset in consensus. Clinical details and demographics were available. The readers noted the presence of pathologic lesions (including local recurrence, lymph nodes, and bone or organ metastases) on the whole-body scan and whether these lesions were not visible on either early or late imaging. To calculate tracer uptake for locally recurring lesions, circular regions of interest were drawn around areas of focally increased uptake on transaxial slices of the prostatic fossa and were automatically adapted to a 3-dimensional volume of interest at a 40% isocontour as previously described (*21*). Care was taken to check that the volume of interest in transverse, coronal, and sagittal slices did not include the bladder. Likewise, a volume of interest was drawn around the bladder using the same method, with care to include only the anatomic bladder as seen on CT imaging. Background uptake was measured in the standard way, using a 1 cm^3 volume of interest in the left gluteal muscle as previously published (*18*).

Statistical Analysis

Bladder (and background gluteal) tracer activity was measured by obtaining the SUV_{mean} (the variable with the lowest coefficient of variation (*2*)). Lesion activity was determined by convention as SUV_{max}. Uptake for the bladder, gluteal musculature, and prostate cancer lesions was compared at 1.5 and 2.5 h by means of the paired Student *t* test; a 2-tailed *P* value of less than 0.05 was considered statistically significant. Protocols were compared for changes in bladder activity using the unpaired Welch *t* test (for unequal sample sizes). The binomial test was used to determine the statistical significance of detection frequency at standard and late imaging. Statistical analyses were performed using SPSS (version 25; IBM) and R (version 4.0.2).

Clinical Follow-up

Rating of lesions as pathologic or benign was confirmed by a composite reference standard as previously published (histology when available, correlative MRI, or a fall in prostate-specific antigen after targeted salvage radiotherapy (*23*)).

RESULTS

Patient Tolerability

All patients were questioned—according to the institutional standard—by a physician before the examination to exclude

TABLE 1
Patient Characteristics

Parameter	Old protocol	New protocol
Age (y)	67.9 ± 6.7	69.2 ± 6.3
Tracer (MBq)	216.9 ± 35.7	243.7 ± 39.5
Gleason score	7 (6–10)	7 (6–9)
Prostate-specific antigen	1.1 ± 32.7 (mean, 11.5)	0.5 ± 45.6 (mean, 7.6)
TNM*	T (1–4) N (0, 0–1) M (0, 0–1)	T (1–4) N (0, 0–1) M (0, 0–1)

*Classification of the Union for International Cancer Control, eighth edition.
Data are median ± SD followed by range in parentheses, unless otherwise noted.

contraindications to forced diuresis by furosemide (e.g., sulfonamide allergy). Patients tolerated both protocols equally well, and no examples of scanner contamination through urinary incontinence were encountered. We found the application of furosemide and oral hydration to be a simple maneuver that was easily integrated into clinical routine.

Changes in Bladder Activity

Greater urinary activity at 2.5 h was seen in the old protocol (7.01 ± 9.03 SUV at 1.5 h vs. 13.42 ± 9.38 SUV at 2.5 h) than in the new protocol (11.04 ± 12.5 SUV at 1.5 h vs. 12.39 ± 13.36 SUV at 2.5 h), as shown in Figure 2. The ratio of bladder activity at 2.5 h to bladder activity at 1.5 h was significantly higher ($P < 0.0001$) for the old protocol (2.33 ± 1.17) than for the new protocol (1.37 ± 0.50).

Changes in Lesion Activity and Tumor-to-Background Ratio (TBR)

For both the old and the new protocols, a significant increase in SUV_{max} for all pathologic lesions was noted from 1.5 to 2.5 h after injection (from 5.98 to 7.78 for the old protocol and from 4.27 to 4.98 for the new protocol, $P < 0.0001$ and $P = 0.02$, respectively). Similarly, TBR for all pathologic lesions (with respect to the gluteal musculature) increased from 1.5 h to 2.5 h (from 55.80 to 91.39 for the old protocol and from 41.88 to 55.96 for the new protocol; $P < 0.0001$ for both; Fig. 3). Comparing the ratio of the TBR at 2.5 h to the TBR at 1.5 h after injection, the mean increase for the old protocol was higher than for the new protocol (1.72 ± 0.56 vs. 1.49 ± 0.62, $P = 0.013$; Fig. 4).

Lesion Detectability

Overall, 71% of patients in the new protocol and 70% in the old protocol had a positive scan (at least 1 pathologic lesion). Comparing the 1.5-h and 2.5-h acquisitions, for the old protocol, 4 patients (4/76 = 5.2% of the patient cohort) had 4 lesions that were visible at the postdiuresis 1.5-h acquisition but not at 2.5 h, having been obscured as a result of the higher bladder activity. Example images are shown in Figure 5. Furthermore, for the old protocol, the lesion SUV_{max} at 2.5 h in 2 cases corresponded almost exactly to the urinary bladder activity. As confirmation, follow-up with the composite standard revealed that 2 of the patients had a subsequent fall in prostate-specific antigen after directed radiotherapy, 1 had correlative MRI findings, and 1 had a prostate-specific antigen fall after systemic therapy.

For the new protocol, 2 patients had additional locally recurrent lesions that could be visualized only at 2.5 h because of increasing tracer uptake. Correlative imaging (the composite standard) was available as confirmation of these 2 lesions. A further 2 patients had lesions that were more clearly visualized at late imaging, delivering greater diagnostic certainty (an example patient image is shown in Supplemental Fig. 1; supplemental materials are available at http://jnm.snmjournals.org).

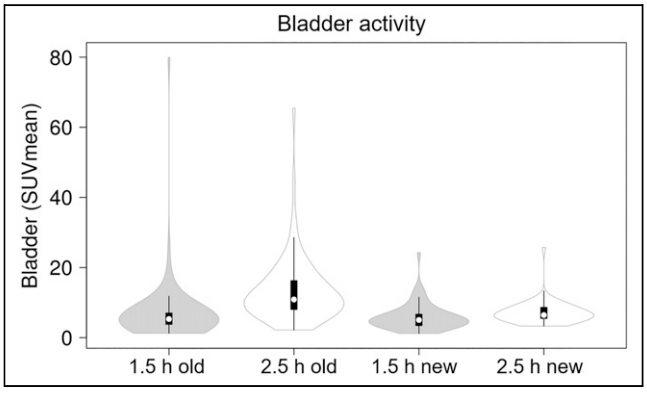

FIGURE 2. Violin plots showing urinary bladder SUV for old and new protocols. Whereas increase in bladder SUV_{mean} is seen for old protocol, this is not the case in new protocol.

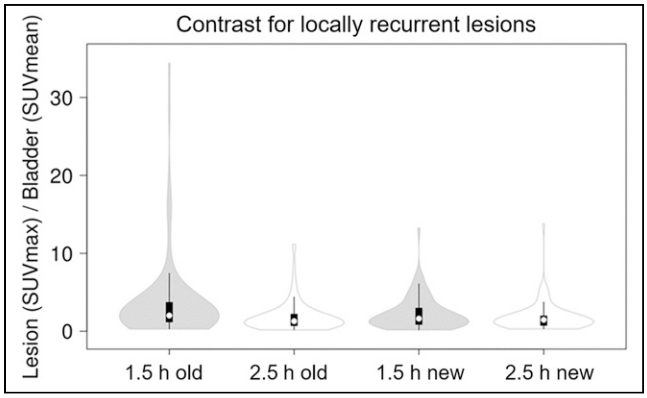

FIGURE 3. Violin plots showing change in locally recurrent lesion SUV_{max} (prostatic fossa/seminal vesicle) vs. bladder SUV_{mean}, that is, lesion-to-bladder contrast. Whereas a decrease in tumor-to-bladder ratio (i.e., lesion visibility) is seen at 2.5 h in old protocol, this was not the case in new protocol.

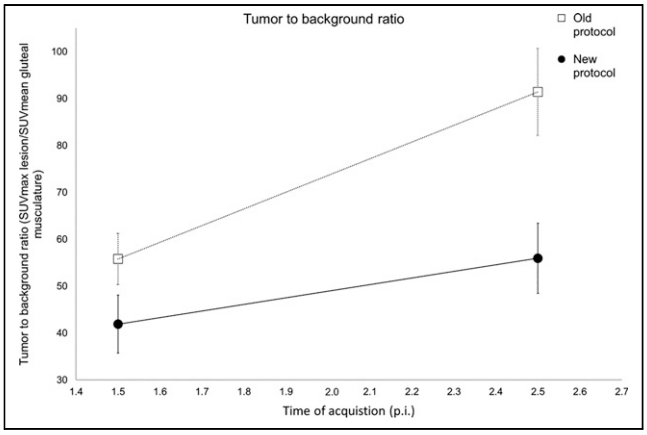

FIGURE 4. TBR change at 1.5 and 2.5 h. Points show mean TBR ± SE. Increase in TBR was lower for new protocol than for old protocol. p.i. = after injection.

DISCUSSION

In this study, we compared two examination protocols that seek to mitigate increased bladder activity through a combination of forced diuresis and additional late imaging. We found that forced diuresis before acquisition of images at 1.5 h after injection gave good results, with resultant low bladder activities and high lesion TBR. Concordant with numerous studies reporting improved lesion detection and visibility at additional late imaging (*2,10–13*), we also found an improved pathologic lesion TBR, with a higher SUV_{max} for most pathologic lesions at additional late imaging. In 2 patients, additional later imaging combined with repeated diuresis revealed 2 lesions that were not visible at early imaging. In 2 patients, 2 lesions were revealed with greater clarity.

Although furosemide produces a prompt onset of diuresis, its biologic half-life is as long as 2 h (*24*). However, our data show that the duration of this residual effect is not sufficient to allow for additional late imaging. In keeping with previous work suggesting that locally recurrent lesions are at risk of being missed because of high bladder activity (*25*), we found that in the old protocol, 4 of 76 patients (5.3%) had lesions that were obscured by increased bladder activity at additional late imaging. Comparing locally recurrent tumor uptake with the local bladder activity confirmed this finding, with lower lesion-to-bladder contrast at late imaging for the old protocol. In contrast, for the new protocol, which includes additional furosemide at late imaging, no reduction in lesion-to-bladder contrast was observed, with all prostate cancer lesions clearly visible at both early and late imaging.

Numerous publications have reported the utility of forced diuresis to mitigate accumulation of bladder activity (*26*). Alternatives, such as the application of intravenous mannitol, have been less well studied (*27*). The current guidelines for PSMA imaging endorse application of furosemide to mitigate activity in the ureters on ^{68}Ga-PSMA-11 PET/CT images (*9*), although application "shortly before or after administration" of the radiopharmaceutical is recommended. Judicious timing of diuresis is essential: Derlin et al. compared 2 protocols with early (concomitant application with radiotracer) and late (100 min after injection) diuresis. Whereas the early protocol resulted in reduced image quality and increased bladder activity, this was not the case for late application (*15*). Likewise, Wondergem et al. advocated application of diuretic shortly before imaging with ^{18}F-DCFPyL (*6*). Piron et al. published results for an optimized protocol for ^{18}F-PSMA-11 with furosemide application 30 min after injection (*28*). The wide variation in protocols and recommendations serves to highlight that the issue remains far from settled and a myriad of protocols advocate both early and dynamic imaging (*29–32*).

We find no publications reporting the influence of forced diuresis on radiotracer uptake: noting the pharmacodynamics of PSMA radioligands, which show increasing radiotracer uptake over time, we posit that forced diuresis might reduce the amount of radiotracer available during this uptake phase; this pharmacokinetic consideration would favor later application over early diuresis (*10,19*). In keeping with this hypothesis, Derlin et al. found reduced image quality after early application of diuretic, although no data for lesion radiotracer uptake were reported (*15*). Early application of the diuretic could result in rapid elimination of the radiotracer during the uptake phase, resulting in reduced lesion uptake. Indeed, our findings suggest that additional diuresis before late imaging results in a lower increase in TBR than was observed in the old protocol. Any protocol must therefore find the optimal balance between improved TBR at later imaging and the short physical half-life of the radiotracer, accumulation of bladder activity, and the ease with which any protocol can be integrated into a busy clinic. Similarly, furosemide should be given when its prompt onset of diuresis has maximum effect; application shortly before or after the radiopharmaceutical is not commensurate with its well-known pharmacodynamics, as is exemplified by our finding that its diuretic effects do not continue into additional late imaging. Application of furosemide

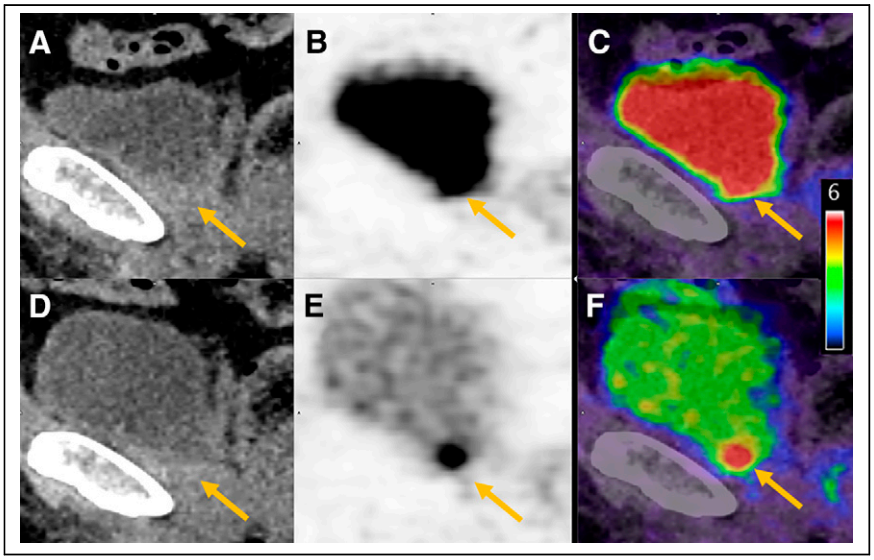

FIGURE 5. Example patient scan showing locally recurrent lesions (arrows) obscured by high bladder activity in old protocol at late imaging. Shown are low-dose CT (A and D), PET (B and E), and fusion of PET and low-dose CT (C and F) images 2.5 h after injection (A–C) and 1.5 h after injection (D–F).

with or shortly after the radiotracer, as recommended by the guidelines (*9*), is therefore unlikely to result in a satisfactory reduction in bladder activity if imaging is performed at 1 h after injection.

Instead, we find our new protocol be a reasonable balance between these myriad competing demands. A larger dose of furosemide (i.e., 20 mg before additional late imaging) is unlikely to be of additional benefit, and Uprimny et al. found no benefit from 40 mg of furosemide compared with 20 mg for imaging 60 min after injection (*33*).

Our results may also find application in PET/MRI (*34*). Because of the halo artifact (*35,36*), optimal reduction of urinary activity is necessary, although the longer examination times encountered in pelvic MRI may necessitate placement of a urinary catheter if forced diuresis shortly before image acquisition is used. Our findings also place new radiotracers into an important context. Recently, PSMA radioligands undergoing biliary or hepatic excretion have been introduced, such as ^{18}F-PSMA-1007 and ^{18}F-rh-PSMA-7 (*8,37*). These cyclotron-produced radiotracers have improved availability and simplify logistic supply chains because of a longer half-life. Other theoretical advantages include a lower positron energy, which may improve imaging resolution (*7,37*). However, the principal clinical advantage of such radiotracers is their low rate of urinary excretion in the first 2 h after injection, with a consequent reduction in bladder activity (*38*). Nevertheless, our data provide insight into the magnitude of any effect size that can be anticipated because of this reportedly favorable pharmacokinetic property. Only a small number of lesions directly contiguous with the bladder or ureter are likely to be obscured, and large patient cohorts would be required to demonstrate this small effect size with adequate power. Neither a matched-pair comparison nor a head-to-head study found any increased detection rate for these new radiotracers (*39,40*), although lower specificity has been observed for ^{18}F-PSMA-1007 (*39*). In contrast, we find that furosemide offers a low-cost, well-tolerated, and easily performed maneuver to reduce urinary activity. Ideally, such protocols would be integrated into any studies comparing tracers undergoing renal extraction and would afford a fair comparison with respect to bladder activity, and consideration must be given to the timing of diuresis when reporting semiquantitative parameters such as lesion SUV.

We note several weaknesses with our study. First, our data were collected retrospectively, and prospective trials are required to confirm the optimum protocol. In keeping with previously published studies (*20*), we sought to establish the utility of our protocol and its effects on urinary bladder activity and lesion uptake. Therefore, the two patient cohorts do not need to be similar with regard to clinical data since these data do not influence the urinary excretion of the tracer. Applied activity was given according to the same weight-adapted dose regime. Despite a slightly greater mean absolute dose of radiopharmaceutical applied in the new protocol, lower bladder activities were seen than with the old protocol (Fig. 2), meaning that the applied activity did not act as a confounder. Lesions classified as pathologic and where discrepancy between the late and early images was noted were confirmed at follow-up by the composite standard. TBR was slightly higher for the old protocol than for the new one on both early and late imaging, reflecting possible underlying differences in patients between these two nonmatched cohorts.

CONCLUSION

Performing ^{68}Ga-PSMA-11 PET/CT at 1.5 h after injection with application of 20 mg of furosemide half an hour before imaging yields good results with excellent TBR and low bladder activity. However, the effect of furosemide does not sufficiently last into additional late imaging, where increased bladder activity, due to diminishing furosemide efficacy, can obscure locally recurrent lesions. To overcome this limitation of the additional late scans, additional furosemide before late imaging provides a useful method to increase the contrast of tumor lesions adjacent to the urinary bladder, allowing for better discrimination of lesions and, in a small number of cases, revealing lesions that were not visible at early imaging. However, additional diuresis for late scans can result in lower increases in tumor radiotracer uptake at late imaging, suggesting that the dose and timing of diuresis can influence the radiotracer's pharmacodynamics.

DISCLOSURE

No potential conflict of interest relevant to this article was reported.

KEY POINTS

QUESTION: Does additional late imaging combined with hydration and diuresis improve local-recurrence visibility in ^{68}Ga-PSMA-11 PET/CT?

PERTINENT FINDINGS: Additional late imaging without furosemide is associated with high bladder activity that obscures locally recurrent lesions. The addition of furosemide and hydration results in lower bladder activity, allowing better discrimination of lesions. In 2 cases, late imaging revealed lesions that were not visible at early imaging.

IMPLICATIONS FOR PATIENT CARE: Later application of furosemide 30 min before imaging is recommended. Additional late imaging should be performed with additional diuresis and hydration.

REFERENCES

1. Afshar-Oromieh A, Holland-Letz T, Giesel FL, et al. Diagnostic performance of ^{68}Ga-PSMA-11 (HBED-CC) PET/CT in patients with recurrent prostate cancer: evaluation in 1007 patients. *Eur J Nucl Med Mol Imaging.* 2017;44:1258–1268.
2. Afshar-Oromieh A, Malcher A, Eder M, et al. PET imaging with a [^{68}Ga]gallium-labelled PSMA ligand for the diagnosis of prostate cancer: biodistribution in humans and first evaluation of tumour lesions. *Eur J Nucl Med Mol Imaging.* 2013;40:486–495.
3. Wondergem M, van der Zant FM, Knol RJJ, Lazarenko SV, Pruim J, de Jong IJ. ^{18}F-DCFPyL PET/CT in the detection of prostate cancer at 60 and 120 minutes: detection rate, image quality, activity kinetics, and biodistribution. *J Nucl Med.* 2017;58:1797–1804.
4. Freitag MT, Radtke JP, Afshar-Oromieh A, et al. Local recurrence of prostate cancer after radical prostatectomy is at risk to be missed in ^{68}Ga-PSMA-11-PET of PET/CT and PET/MRI: comparison with mpMRI integrated in simultaneous PET/MRI. *Eur J Nucl Med Mol Imaging.* 2017;44:776–787.
5. Heusser T, Mann P, Rank CM, et al. Investigation of the halo-artifact in ^{68}Ga-PSMA-11-PET/MRI. *PLoS One.* 2017;12:e0183329.
6. Wondergem M, van der Zant FM, Rafimanesh-Sadr L, Knol RJJ. Effect of forced diuresis during ^{18}F-DCFPyL PET/CT in patients with prostate cancer: activity in ureters, kidneys and bladder and occurrence of halo artefacts around kidneys and bladder. *Nucl Med Commun.* 2019;40:652–656.
7. Rahbar K, Afshar-Oromieh A, Bogemann M, et al. ^{18}F-PSMA-1007 PET/CT at 60 and 120 minutes in patients with prostate cancer: biodistribution, tumour detection and activity kinetics. *Eur J Nucl Med Mol Imaging.* 2018;45:1329–1334.
8. Eiber M, Kroenke M, Wurzer A, et al. ^{18}F-rhPSMA-7 PET for the detection of biochemical recurrence of prostate cancer after radical prostatectomy. *J Nucl Med.* 2020;61:696–701.

9. Fendler WP, Eiber M, Beheshti M, et al. ^{68}Ga-PSMA PET/CT: joint EANM and SNMMI procedure guideline for prostate cancer imaging—version 1.0. *Eur J Nucl Med Mol Imaging.* 2017;44:1014–1024.
10. Afshar-Oromieh A, Sattler LP, Mier W, et al. The clinical impact of additional late PET/CT imaging with ^{68}Ga-PSMA-11 (HBED-CC) in the diagnosis of prostate cancer. *J Nucl Med.* 2017;58:750–755.
11. Sahlmann C-O, Meller B, Bouter C, et al. Biphasic ^{68}Ga-PSMA-HBED-CC-PET/CT in patients with recurrent and high-risk prostate carcinoma. *Eur J Nucl Med Mol Imaging.* 2016;43:898–905.
12. Afshar-Oromieh A, Sattler LP, Steiger K, et al. Tracer uptake in mediastinal and paraaortal thoracic lymph nodes as a potential pitfall in image interpretation of PSMA ligand PET/CT. *Eur J Nucl Med Mol Imaging.* 2018;45:1179–1187.
13. Hohberg M, Kobe C, Täger P, et al. Combined early and late [^{68}Ga]PSMA-HBED-CC PET scans improve lesion detectability in biochemical recurrence of prostate cancer with low PSA levels. *Mol Imaging Biol.* 2019;21:558–566.
14. Fennessy N, Lee J, Shin J, et al. Frusemide aids diagnostic interpretation of ^{68}Ga-PSMA positron emission tomography/CT in men with prostate cancer. *J Med Imaging Radiat Oncol.* 2017;61:739–744.
15. Derlin T, Weiberg D, von Klot C, et al. ^{68}Ga-PSMA I&T PET/CT for assessment of prostate cancer: evaluation of image quality after forced diuresis and delayed imaging. *Eur Radiol.* 2016;26:4345–4353.
16. Schmuck S, Nordlohne S, von Klot CA, et al. Comparison of standard and delayed imaging to improve the detection rate of [^{68}Ga]PSMA I&T PET/CT in patients with biochemical recurrence or prostate-specific antigen persistence after primary therapy for prostate cancer. *Eur J Nucl Med Mol Imaging.* 2017;44:960–968.
17. Alberts I, Sachpekidis C, Gourni E, et al. Dynamic patterns of [^{68}Ga]Ga-PSMA-11 uptake in recurrent prostate cancer lesions. *Eur J Nucl Med Mol Imaging.* 2020;47:160–167.
18. Alberts I, Sachpekidis C, Dijkstra L, et al. The role of additional late PSMA-ligand PET/CT in the differentiation between lymph node metastases and ganglia. *Eur J Nucl Med Mol Imaging.* 2020;47:642–651.
19. Afshar-Oromieh A, Hetzheim H, Kubler W, et al. Radiation dosimetry of ^{68}Ga-PSMA-11 (HBED-CC) and preliminary evaluation of optimal imaging timing. *Eur J Nucl Med Mol Imaging.* 2016;43:1611–1620.
20. Haupt F, Dijkstra L, Alberts I, et al. ^{68}Ga-PSMA-11 PET/CT in patients with recurrent prostate cancer: a modified protocol compared with the common protocol. *Eur J Nucl Med Mol Imaging.* 2020;47:624–631.
21. Afshar-Oromieh A, Avtzi E, Giesel FL, et al. The diagnostic value of PET/CT imaging with the ^{68}Ga-labelled PSMA ligand HBED-CC in the diagnosis of recurrent prostate cancer. *Eur J Nucl Med Mol Imaging.* 2015;42:197–209.
22. Eder M, Neels O, Muller M, et al. Novel preclinical and radiopharmaceutical aspects of [^{68}Ga]Ga-PSMA-HBED-CC: a new PET tracer for imaging of prostate cancer. *Pharmaceuticals (Basel).* 2014;7:779–796.
23. Alberts I, Prenosil G, Sachpekidis C, et al. Digital versus analogue PET in [^{68}Ga]Ga-PSMA-11 PET/CT for recurrent prostate cancer: a matched-pair comparison. *Eur J Nucl Med Mol Imaging.* 2020;47:614–623.
24. Ponto LL, Schoenwald RD. Furosemide (frusemide): a pharmacokinetic/pharmacodynamic review (part I). *Clin Pharmacokinet.* 1990;18:381–408.
25. Freitag MT, Radtke JP, Afshar-Oromieh A, et al. Local recurrence of prostate cancer after radical prostatectomy is at risk to be missed in ^{68}Ga-PSMA-11-PET of PET/CT and PET/MRI: comparison with mpMRI integrated in simultaneous PET/MRI. *Eur J Nucl Med Mol Imaging.* 2017;44:776–787.
26. Sheikhbahaei S, Afshar-Oromieh A, Eiber M, et al. Pearls and pitfalls in clinical interpretation of prostate-specific membrane antigen (PSMA)-targeted PET imaging. *Eur J Nucl Med Mol Imaging.* 2017;44:2117–2136.
27. Matteucci F, Mezzenga E, Caroli P, et al. Reduction of ^{68}Ga-PSMA renal uptake with mannitol infusion: preliminary results. *Eur J Nucl Med Mol Imaging.* 2017;44:2189–2194.
28. Piron S, De Man K, Schelfhout V, et al. Optimization of PET protocol and interrater reliability of ^{18}F-PSMA-11 imaging of prostate cancer. *EJNMMI Res.* 2020;10:14.
29. Sachpekidis C, Kopka K, Eder M, et al. ^{68}Ga-PSMA-11 dynamic PET/CT imaging in primary prostate cancer. *Clin Nucl Med.* 2016;41:e473–e479.
30. Uprimny C, Kroiss AS, Decristoforo C, et al. Early dynamic imaging in ^{68}Ga-PSMA-11 PET/CT allows discrimination of urinary bladder activity and prostate cancer lesions. *Eur J Nucl Med Mol Imaging.* 2017;44:765–775.
31. Varasteh Z, Mohanta S, Robu S, et al. Molecular imaging of fibroblast activity after myocardial infarction using a ^{68}Ga-labeled fibroblast activation protein inhibitor, FAPI-04. *J Nucl Med.* 2019;60:1743–1749.
32. Beheshti M, Paymani Z, Brilhante J, et al. Optimal time-point for ^{68}Ga-PSMA-11 PET/CT imaging in assessment of prostate cancer: feasibility of sterile cold-kit tracer preparation? *Eur J Nucl Med Mol Imaging.* 2018;45:1188–1196.
33. Uprimny C, Bayerschmidt S, Kroiss AS, et al. Impact of forced diuresis with furosemide and hydration on the halo artefact and intensity of tracer accumulation in the urinary bladder and kidneys on [^{68}Ga]Ga-PSMA-11-PET/CT in the evaluation of prostate cancer patients. *Eur J Nucl Med Mol Imaging.* 2021;48:123–133.
34. Li M, Huang Z, Yu H, Wang Y, Zhang Y, Song B. Comparison of PET/MRI with multiparametric MRI in diagnosis of primary prostate cancer: a meta-analysis. *Eur J Radiol.* 2019;113:225–231.
35. Afshar-Oromieh A, Haberkorn U, Schlemmer HP, et al. Comparison of PET/CT and PET/MRI hybrid systems using a ^{68}Ga-labelled PSMA ligand for the diagnosis of recurrent prostate cancer: initial experience. *Eur J Nucl Med Mol Imaging.* 2014;41:887–897.
36. Afshar-Oromieh A, Wolf M, Haberkorn U, et al. Effects of arm truncation on the appearance of the halo artifact in ^{68}Ga-PSMA-11 (HBED-CC) PET/MRI. *Eur J Nucl Med Mol Imaging.* 2017;44:1636–1646.
37. Rahbar K, Afshar-Oromieh A, Seifert R, et al. Diagnostic performance of ^{18}F-PSMA-1007 PET/CT in patients with biochemical recurrent prostate cancer. *Eur J Nucl Med Mol Imaging.* 2018;45:2055–2061.
38. Rahbar K, Weckesser M, Ahmadzadehfar H, Schafers M, Stegger L, Bogemann M. Advantage of ^{18}F-PSMA-1007 over ^{68}Ga-PSMA-11 PET imaging for differentiation of local recurrence vs. urinary tracer excretion. *Eur J Nucl Med Mol Imaging.* 2018;45:1076–1077.
39. Rauscher I, Krönke M, König M, et al. Matched-pair comparison of ^{68}Ga-PSMA-11 PET/CT and ^{18}F-PSMA-1007 PET/CT: frequency of pitfalls and detection efficacy in biochemical recurrence after radical prostatectomy. *J Nucl Med.* 2020;61:51–57.
40. Kuten J, Fahoum I, Savin Z, Shamni O, et al. Head-to-head comparison of ^{68}Ga-PSMA-11 with ^{18}F-PSMA-1007 PET/CT in staging prostate cancer using histopathology and immunohistochemical analysis as a reference standard. *J Nucl Med.* 2020;61:527–532.